Black weathering of Bentheim and Obernkirchen sandstone

Timo G. Nijland[1], C. Wim Dubelaar[2], Rob P.J. van Hees[1,3] & Thomas J.M. van der Linden[1]

[1] TNO Building & Construction Research, Delft
[2] TNO-NITG Netherlands Institute of Applied Geosciences, Utrecht
[3] Delft University of Technology, Faculty of Architecture, Delft

Black weathering of sandstone in monuments is widespread. Some objects owe their name to it, like the Porta Nigra in Trier (Germany). Other than the black gypsum crusts common on limestone, the black weathering layer on sandstone is rather thin and well adherent. Formation of such layers on Bentheim and Obernkirchen sandstone, both widely used in the Netherlands, has been investigated by microscopy and whole rock chemistry. Samples were obtained from several monuments in the Netherlands, amongst them the Old and New Church (Delft), St. John's cathedral ('s Hertogenbosch) and St. Plechelmus' basilica (Oldenzaal). Microscopically, the layers are composed of algae and fungi, gypsum, airborne particles such as fly ash, and iron (hydr)oxides, present on the surface and in directly adjacent pores. Gypsum is present in all samples, algae are not, but typically occur in the most black-ish layers. Black layers show significant increases in loss on ignition (LOI), total and organic carbon, total sulfur and iron, as well as Pb, Cu, Zn and Sn. Formation of thin black layers is evidently not due to a single process, but involves formation of gypsum, deposition of airborne material, microbiotic activity and dissolution and redeposition of Fe-(hydr)oxides.

Key words: Natural stone, Bentheim sandstone, Obernkirchen sandstone, black weathering, algae, gypsum, microscopy

1   Introduction

Sandstone imported from Germany has been applied as dimension and ornamental stone in Dutch monuments from the 11th or 12th century onward. These include Buntsandstein from the Weser and Main areas, known as 'Wezerzandsteen' or 'rode Bremer zandsteen', and, especially, Bentheim and Obernkirchen sandstone (Slinger et al., 1980). Several types of sandstone used as building stone, including the Bentheim and Obernkirchen, exhibit distinct, thin black weathering layers. This is often experienced as non-aesthetic by the general public, but the decision whether cleaning is desirable and allowable, is one with both technological (How ? What is the effect on durability ?) and ethical (Are original parts of the stone removed ? Will historical information be lost ?) dimensions (e.g. Van Bommel 2001). Both aspects can only be fully considered if the underlying scientific question is answered: Which components are present in the thin black weathering layers and which processes are responsible for their formation ?

Together, studies on the origin of colored weathering layers, often called *patina*, on natural stone used as building stone, would fill a library of considerable size. Generalizing, two groups of hypotheses have been proposed, i.e. a microbiotic origin (e.g. Krumbein 1992) or derivation from historic surface treatments. Arguments and counterarguments for both hypotheses have been summarized by Vendrell-Saz et al. (1996) and Dubelaar et al. (2003).

Thin, black weathering layers on sandstones form a specific catergory (e.g. Bluck & Porter 1991ab). Dissolution and precipitation processes are likely to occur in porous sandstones, and may be responsible for iron enrichment (Becker 1987, Dubelaar 1990) and formation of new Fe-minerals such as pyrite, rozenite, jarosite, ferrihydrite and goethite (Nord & Tronner 1991, 1992). Enrichment of heavy minerals are observed (e.g. McDonnell et al. 1991, Nord & Tronner 1991, 1992), as are the presence of airborne particles, such as fly ash (Dubelaar & Pieters 1992, Gisbert et al. 1996).
The contribution by microbiota is often neglected, but was studied in detail by Young (1997).

Gypsum is presumably an important component of thin black weathering layers on sandstone, as with many natural stones, notable calcareous ones. It is commonly attributed to SO_2 derived from air pollution or SO_4^{2-} from mortars, but the presence of fly ash may also play a role. Ausset et al. (2000) demonstrated that the presence of fly ash on the surface of limestones resulted in larger amounts of gypsum to be formed, as well as its formation at deeper levels in the stone; a similar mechanism was observed by Esbert et al. (1996) on limestones from the cathedral of Burgos.

Fig. 1. Part of the façade of St. John's cathedral, 's Hertogenbosch, built in Bentheim sandstone. Note the variable intensity of black weathering. Samples Z1 and Z2 (Table 2) have been collected from this façade.

In the Dutch situation, Bentheim and Obernkirchen sandstone ofter show more intense black weathering than other sandstones used, though considerable variation occurs, even between sandstones brought into the same façade in the same period (Fig. 1). Only two unpublished studies by McDonnell et al. (1991) and Dubelaar & Pieters (1992) were available for these sandstones. Given the large variation in exposure conditions, degrees and amounts of air pollution and types of sandstone, study of the situation in the Netherlands was deemed necessary by conservation authorities.

2 Petrographic characteristics and use of Bentheim and Obernkirchen sandstone

2.1 Bentheim sandstone

The Bentheim sandstone is a well-sorted, medium-grained (typically 0.1- 0.2 mm) marine sandstone deposited in the Lower Saxonian basin during the Valanginien (Lower Cretaceous), occuring at or near the surface in the Dutch – German border region near Bad Bentheim. The sandstone consists of > 90 vol.% quartz, with accessory feldspars, heavy minerals (tourmaline, zircon, rutile) and Fe-(hydr)oxides, and is, at the localities where it has been quarried as a building stone, almost devoid of clay minerals and carbonates (Füchtbauer 1955, Kemper 1976, Becker 1987; Table 1).

In the Netherlands, Bentheim sandstone was applied as a building stone in the Twenthe region from the 12th century onwards, appearing outside that region at the end of the 14th century. From that time, the requirement of toll on the shipping routes for Drachenfels trachyte and Rhenish tuffs used in older monuments greatly enhanced the use of Bentheimer sandstone, which could be imported along toll-free routes (Slinger et al. 1980). It was applied on the Dom church in Utrecht in 1450; afterwards, use spread rapidly, even in the west of the country (though here, it was first transported to the workshops of the Keldermans family in Malines (Mechelen) in Flanders, Belgium, and then to many cities in Holland and Zeeland in the Netherlands (Slinger et al. 1980). Other monuments built with Bentheim sandstone include the tower of the New Church in Delft (1494-1495), St. John's cathedral, 's Hertogenbosch, the former town hall, presently Royal Palace (applied there from 1648 onwards), and house of the brothers Tripp, presently seat of the Royal Netherlands Academy of Science (1660-1662), in Amsterdam.

2.2 Obernkirchen sandstone

The Obernkirchen sandstone has also been deposited in the Lower Saxionan basin, but is slightly younger (Wealden). It has been and still is quarried at the Bückeberg, west of Hannover, Germany. It is a light grey to yellowish fine-grained, moderately to well-sorted sandstone, composed of quartz and rock fragments up to 0.15 mm, with minor amounts of mica, heavy minerals and Fe-(hydr)oxides and rare feldspars (Chitsazian 1985; Table 1). The Obernkirchen sandstone contains about 15 % of cement, mainly quartz and kaolinite / illite.

In the Netherlands, Obernkirchen sandstone was only scarcely applied during the period of Gothic architecture, notably at the Martinitower in Groningen (1469). During the 17th century Renaissance period, it became more widely used (Slinger et al. 1980). Monuments built with Obernkirchener sandstone include the the former town hall, presently Royal Palace, in Amsterdam (from 1648 onwards), the town halls of Leiden (1596-1597) and Delft (1618-1620), and the International Court of Justice in The Hague (1909-1913).

3   Analytical methods

Samples of several monuments showing variable degrees of black weathering, i.e. from light grey to lesser or more intense black, have been studied by a combination of polarization-and-fluorescence microscopy (PFM) and scanning electron microscopy (SEM). From a selection of samples, black weathering layer and interior were carefully separated for whole rock chemistry. Major and trace element compositions have been determined by both X-ray fluorescence spectrometry (XRF) and inductively coupled plasma – mass spectrometry (ICP-MS). Loss on ignition (LOI) was determined gravimetrically at different temperatures (105, 450, 550, 800 and 1000 °C), whereas total and organic carbon and total sulfur contents were determined by Leco method. ICP-MS analyses were also performed on a partial extraction of the powders, using oxalic acid. An overview of samples studied is given in Table 2. More detailed descriptions of the monuments from which they have been obtained, history of the specific samples and macroscopic description have been reported by Dubelaar et al. (2003).

Table 1. Mineralogical composition and physical properties of Bentheim (Füchtbauer 1955, Kemper 1976, Becker 1987, Grimm 1990) and Obernkirchen sandstone (Chitsazian 1985, Grimm 1990).

		Bentheim	Obernkirchen	
Clasts and detrital minerals	Quartz	> 90	76	vol. %
	Rock fragments		6.6	vol. %
	Mica		0.8	vol. %
	Feldspar	acc.	0.2	vol. %
	Heavy minerals	acc.	0.9	vol. %
Secondary minerals in pores	Quartz		4.8	vol. %
	Clay minerals	acc.	5.0	vol. %
	Fe-(hydr)oxides		5.4	vol. %
	Anhydrite	acc.		vol. %
	Anatase	acc.		vol. %
Density		2.04	2.11	g cm^{-3}
Grain size		0.1 – 0.5	0.04 – 0.15	mm
Porosity		21 – 32	16 – 21	vol. %
Specific surface area		1.69	1.23	m^2 g^{-1}

Table 2. Samples studied.

Code	Sandstone	Source	Age
Z1	Bentheim	St. John's cathedral, 's Hertogenbosch	19th century restoration
Z2	Bentheim	St. John's cathedral, 's Hertogenbosch	19th century restoration
Z3	Bentheim	unknown monument, Utrecht	unknown
Z4	Bentheim	St. Plechelmus' basilica, Oldenzaal	19th century restoration
Z5	Bentheim	Old Church, Delft	presumed 1450
Z6	Obernkirchen	Royal Palace, Amsterdam	1656
Z7	Bentheim	New Church, Delft	presumed 1486
Z8	Obernkirchen	unknown monument	probably 17th century
Z9	Bentheim ?	New Church, Delft	presumed 1486

4 Polarization-and-fluorescence microscopy of black weathering layer

The thickness of black weathering layers on Bentheim and Obernkirchen sandstone varies from about 0.1 to a few mm. UV-fluorescence microscopy clearly shows that the thin black layers are thin indeed, i.e. 1 – 3 quartz grains thick, but also rather dense, thus 'sealing' the interior of the porous sandstones (Fig. 2). Composition of the layers is variable. Gypsum is always present, and fixates fly ash, soot and other airborne particles (Fig. 3), whereas occasionally, it also forms a replacing cement (Fig. 4), keeping the quartz grains near the surface in place. The various airborne particles encapsulated by the gypsum are in part responsible for the black appearance. In addition to gypsum, micro-organisms or their remains form part of several of the thin black layers (Fig. 5). The latter in part developed on top of pores, filled with remains of precursor organisms, and are surrounded by a brownish, semi-opaque layer (Fig. 5). Local carbonate crusts may also be present.
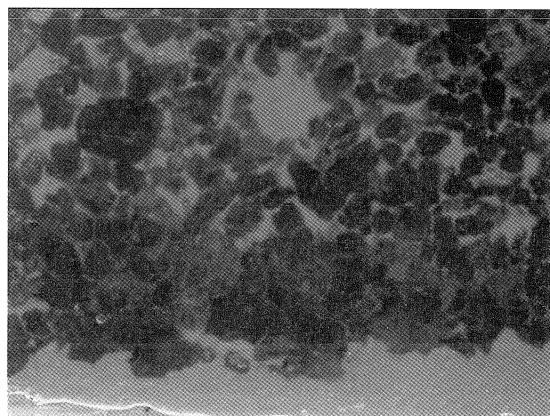

Fig. 2. UV-fluorescence microphotograph of a section perpendicular to the black weathering layer on Bentheim sandstone from St. John's cathedral, 's Hertogenbosch (view 2.7 x 1.8 mm). Note the strong decrease of porosity in the black weathering layer at the bottom.
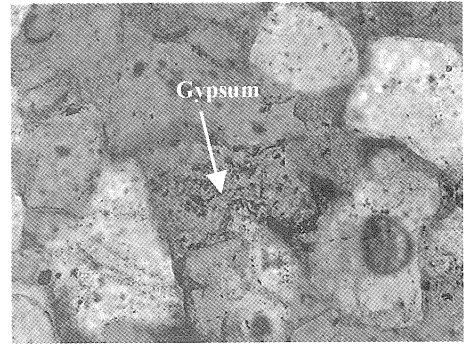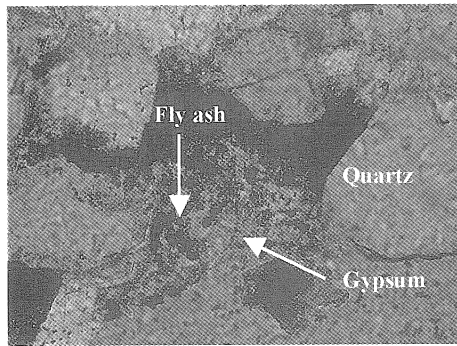
Fig. 3. Microphotograph showing gypsum, encapsulating various airborne particles in the black weathering layer on Bentheim sandstone from, left, St. John's cathedral, 's Hertogenbosch (perpendicular section, view 0.7 x 0.45 mm), and, right, St. Plechelmus' basilica, Oldenzaal (parallel section, view 0.7 x 0.45 mm).
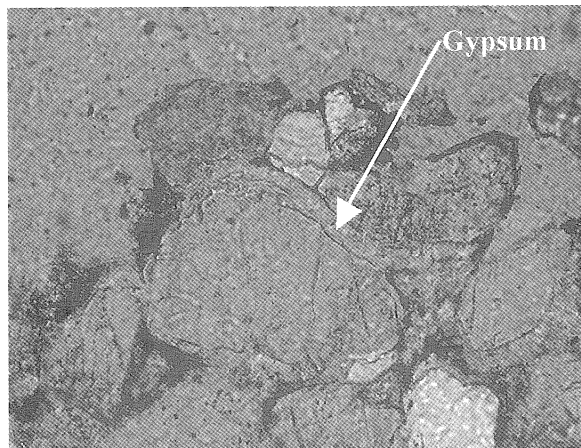
Fig. 4. Microphotograph showing gypsum as replacing cement in the black weathering layer on Bentheim sandstone from St. John's cathedral, 's Hertogenbosch (perpendicular section, view 1.4 x 0.9 mm).
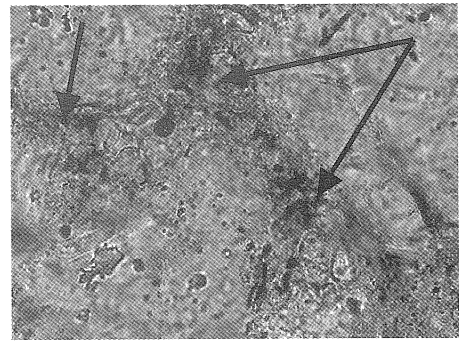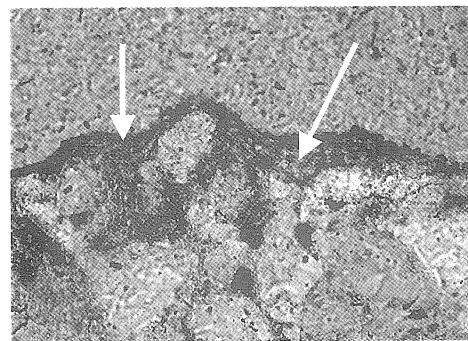

Fig. 5. Microphotograph showing algae on, left, Obernkirchen sandstone from an unknown monument (perpendicular section, view 0.7 x 0.45 mm) and, right, Bentheim sandstone from St. John's cathedral, 's Hertogenbosch (parallel section, view 0.35 x 0.22 mm).

5   Scanning electron microscopy

SEM observations confirm those by PFM and show gypsum crystals with various habits to be a major component in the black weathering layers; occasionally, several generations of gypsum may be distinguished (Fig. 6). In some cases, gypsum shows clear dissolution features. The presence of algae too, was confirmed by SEM; in addition, fungi have been observed in the black weathering layers of two samples. Energy dispersive spectroscopic analyses (EDS) show that in some cases, the black weathering layers are enriched in Pb, Cu, Zn, Cl and P (Fig. 7). Pb may be present both as anglesite or as metallic lead (Fig. 8). In some cases, these enrichments could be attributed to the presence of non-ferro metal building elements, such as the presence of lead joints between the sandstone blocks in case of the metallic lead. In other cases, both air pollution and chemical remnants of ancient coatings are possible sources. In one case (Old Church, Delft), the water soluble salts halite and glauberite have been observed on top of the black weathering layer (Fig. 9). They are considered to be a non-permanent feature, probably aerosol from sea.
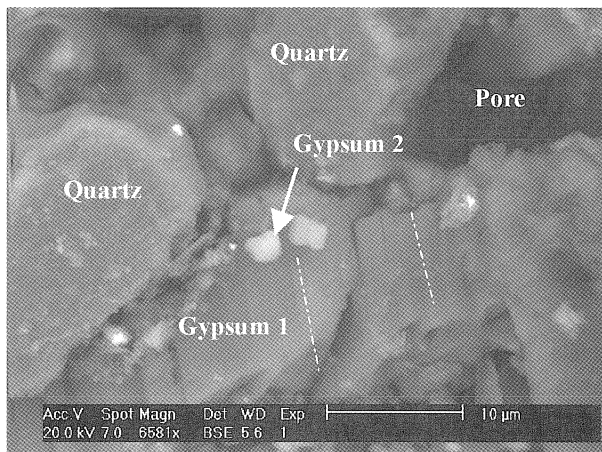
Fig. 6. SEM microphotograph showing two generations of gypsum in the black weathering layer on Bentheim sandstone from St. Plechelmus' basilica, Oldenzaal.
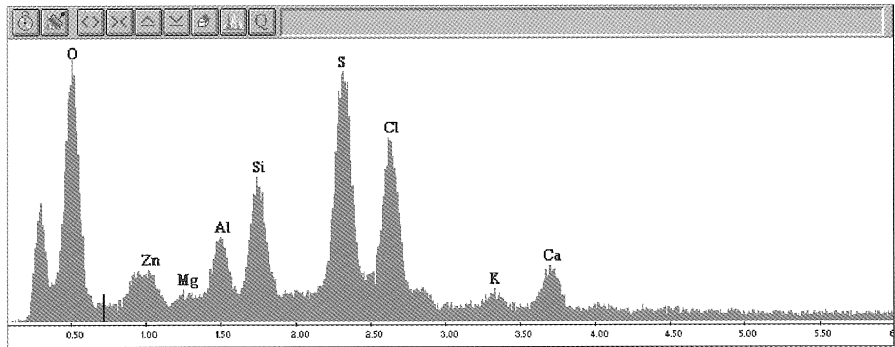
Fig. 7a. EDS spectrum of the surface of a feldspar grain in the black weathering layer on Bentheim sandstone from St. Plechelmus' basilica, Oldenzaal. Note the enrichment in Zn and Cl besides S.

Fig. 7b. EDS spectrum of the surface of a quartz grain in the black weathering layer on Bentheim (?) sandstone from the New Church, Delft. Note the enrichment in Pb, Zn and P.

Fig. 8. Metalic lead in the black weathering layer on Bentheim sandstone from St. Plechelmus' basilica, Oldenzaal.

186

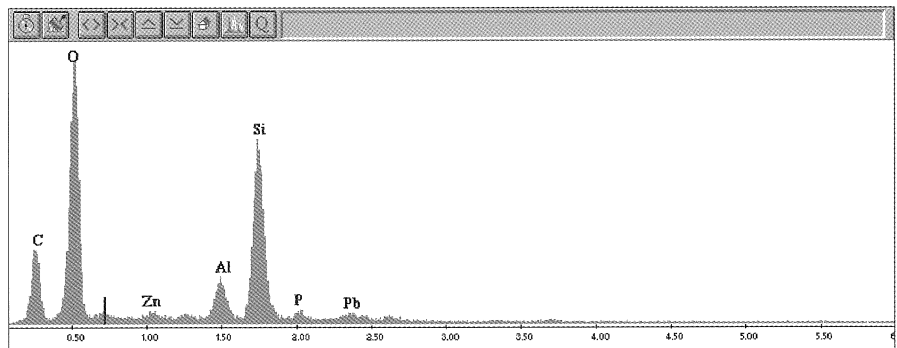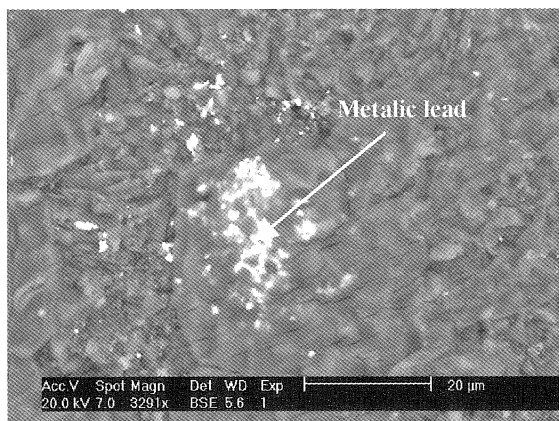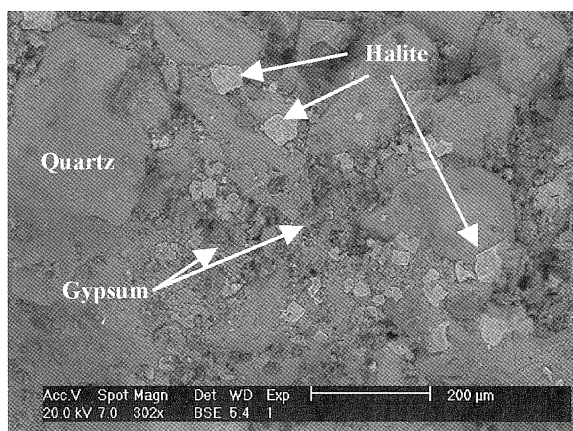*Fig. 9. SEM microphotograph showing halite crystals on top of the black weathering layer on Bentheim sandstone from the Old Church, Delft.*

Table 3. Loss on ignition (LOI; wt.%), total and organic carbon and total sulfur contents (ppm) of the black weathering layer (BWL) and substrate (Subs). For sample codes, see Table 2.

		Z1		Z2		Z3		Z4		Z8	
		BLW	Subs	BWL	Subs	BWL	Subs	BWL	Subs	BWL	Subs
LOI	105 °C	4.456	3.473	7.125	2.826	7.19	3.237	4.636	1.536	4.24	0.151
LOI	450 °C	1.301	0.041	0.344	0.077	0.681	0.048	0.891	0.161	0.795	0.161
LOI	550 °C	0.154	0.094	0.138	0.122	0.271	0.125	0.257	0.238	0.443	0.402
LOI	800 °C	0.194	0.139	0.317	0.291	0.2	0.22	0.186	0.182	0.478	0.476
LOI	1000 °C	0.048	0.021	0.025	0.021	0.032	0.02	0.094	0.02	0.06	0.048
Organic carbon		0.339	0.001	0.042	0.017	0.329	0.018	0.107	0.037	0.43	0.044
Total carbon		0.398	0.015	0.041	0.019	0.377	0.027	0.13	nd	0.451	0.049
Total sulfur		0.569	0.004	0.214	0.023	0.011	0.001	0.38	0.005	0.013	0.003

6   Whole rock chemistry

All samples show an increase in LOI at all temperatures (105, 450, 550, 800 and 1000 °C), organic and total carbon, and total sulfur contents in the black weathering layer compared to the substrate (Table 3). The increase in LOI reflects several components of the black layer: LOI at 105 °C can be attributed to physically bound water, and, possibly, water in organic components. LOI at 450 °C reflects, in part, the decomposition of gypsum at 163 °C. Phases responsible for LOI at 550 and 800 °C are less easily identified, but LOI at 1000 °C may represent breakdown of small amounts of carbonates between 800 and 950 °C. Total and organic carbon are enriched in the black weathering layer relative to the substrate; organic carbon is by far the largest fraction of carbon present (Table 3) and reflects microbiotic components as well as organic matter from air pollution. Enrichment in S reflects formation of gypsum, but low S contents in samples Z3 and Z8 (Table 3) show that only minor amounts of gypsum are present in some black weathering layers, i.e. only small amounts of gypsum are necessary to fixate airborne particles responsible for the blackish appearance.

Iron is also increased in the black weathering layer compared to the substrate; both total iron contents and oxalic acid soluble (i.e. easily available) iron are enriched in the black weathering layer (Fig. 10, Tables 4 – 5 and 6, respectively). Enrichment in both total and oxalic acid soluble Fe (Fig. 10) shows that not only the total Fe content of the black weathering layers is increased, but that the speciation of Fe also changed during the enrichment process, more relatively mobile Fe being present in the black weathering layer. To a lesser extent, heavy metals such as Pb, Cu, Zn and Sn also show an increase in the black weathering layer (Tables 4 – 6); this with exception of one sample, in which the high Pb content in the substrate may be due to accessory galena). Enrichment factors are presented in Table 7 and Fig. 11. For the enrichment in heavy metals, several sources may be present, viz. air pollution, non-ferro building elements, dissolution & precipitation processes and, possibly, historic surface treatments.
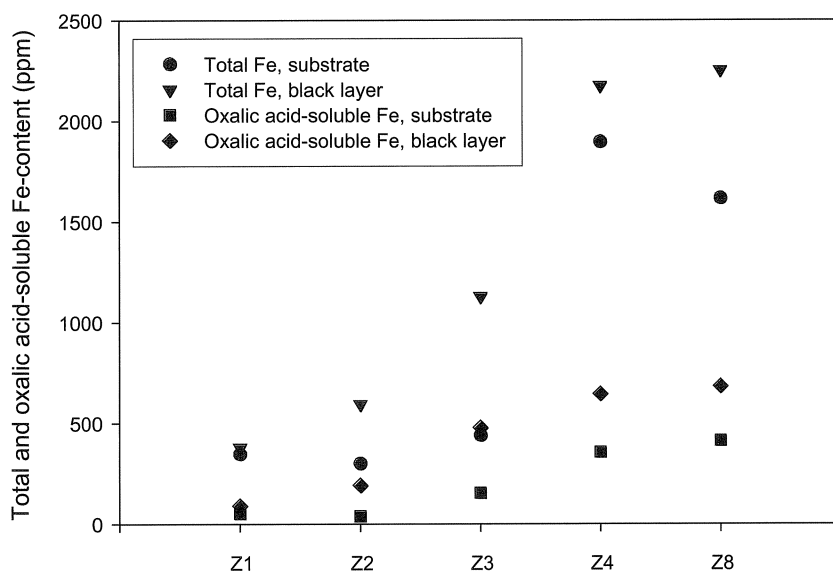

Fig. 10. Total and oxalic acid soluble Fe-contents in the black weathering layer and the substrate, showing enrichment of the former. For sample codes, see Table 2.

Table 4. Whole rock chemical compositions of the black weathering layer (BWL) and substrate (Subs) as determined by XRF. Major elements as oxides in wt. %, trace elements in ppm; dl = detection limit.

Sample	Z1		Z2		Z3		Z4		Z8	
	BWL	Subs	BWL	Subs	BWL	Subs	BWL	Subs	BWL	Subs
SiO_2	90.69	94.38	92.66	93.09	92.63	93.37	90.21	90.56	89.63	90.56
TiO_2	0.046	0.044	0.062	0.059	0.069	0.073	0.091	0.134	0.400	0.343
Al_2O_3	1.00	1.00	1.37	1.38	1.54	1.48	1.90	1.82	3.62	3.53
Fe_2O_3	0	0	0	0	0.02	0	0.17	0.14	0.19	0.10
MnO	0	0	0	0	0	0	0.001	0.001	0.001	0
MgO	0	0	0	0	0	0	0	0	0	0.01
CaO	0.77	0	0.38	0.10	0.07	0.03	0.57	0.01	0.04	0.06
Na_2O	0.09	0.10	0.08	0.08	0.08	0.07	0.08	0.07	0.15	0.13
K_2O	0.23	0.25	0.05	0.05	0.26	0.25	0.26	0.26	0.25	0.24
P_2O_5	0.029	0.004	0.008	0.006	0.017	0.003	0.010	0.007	0.060	0.058
S	0.77	0.00	0.32	0.09	0	0.01	0.57	0	0.01	0.03
Total	93.64	95.78	94.92	94.85	94.69	95.30	95.31	95.24	96.13	96.15
Sc	1	dl	2	1	2	2	12	2	6	1
V	6	7	6	6	16	9	12	14	21	18
Cr	10	8	11	8	12	10	15	21	42	30
Ni	dl	dl	dl	dl	dl	dl	2	dl	4	2
Cu	14	5	12	5	14	4	345	6	7	23
Zn	6	dl	10	1	315	19	167	45	21	18
Ga	1	1	1	dl	dl	1	1	3	dl	dl
As	dl	dl	dl	dl	dl	1	9	dl	1	1
Rb	7	7	4	3	9	8	9	8	12	12
Sr	35	10	21	11	15	12	29	12	121	151
Y	2	2	4	4	dl	3	3	4	28	22
Zr	43	38	38	38	39	46	54	85	1154	746
Nb	2	2	3	3	2	3	5	4	9	8
Sn	4	1	dl	2	5	3	6	1	3	2
Ba	79	80	48	39	99	93	91	87	166	69
La	4	5	5	5	6	6	6	6	45	56
Nd	6	6	8	9	8	5	9	7	67	76
Pb	86	106	100	13	1023	41	214	146	213	34
Th	3	3	2	4	10	3	2	3	15	11
U	dl	1	1	dl	5	2	dl	dl	3	2

Table 5. Whole rock chemical compositions of the black weathering layer (BWL) and substrate (Subs.) as determined by ICP-MS. Elements in ppm; dl = detection limit.

Sample	Z1		Z2		Z3		Z4		Z8	
	BWL	Subs	BWL	Subs	BWL	Subs	BWL	Subs	BWL	Subs
Li	5.8	7.6	3.7	4.0	7.3	6.4	7.2	5.8	8.4	8.6
Na	276	636	163	167	143	111	169	114	546	537
Mg	93	237	94	65	102	56	177	125	291	237
Al	5294	7195	5086	5480	5973	5502	6933	6343	11464	12237
K	2813	2961	471	371	1942	2046	2272	1811	1864	1872
Ca	9445	8052	2997	590	702	165	4936	175	457	331
Sc	0.4	0.5	0.6	1.0	0.8	0.7	2.1	1.2	2.5	2.0
Ti	355	276	354	392	358	414	426	724	2204	1950
V	3.8	4.7	4.8	4.3	14	5.6	9.4	9.5	17	13
Cr	1.6	1.7	2.1	1.6	1.8	1.6	2.5	2.6	4.1	3.4
Mn	3.6	5.4	5.8	2.3	9.1	2.4	11	11	13	6.5
Fe	379	348	594	301	1129	441	2174	1896	2251	1617
Ni	2.3	3.4	3.9	2.4	3.4	2.4	3.3	3.4	5.2	4.2
Cu	22	17	15	6.7	15	5.1	352	6.5	11	6.4
Zn	111	585	25	23	317	31	174	37	32	17
Ga	1.5	2.2	0.6	0.5	1.4	1.2	1.5	1.2	2.9	1.7
As	1.6	1.7	1.3	0.7	5.3	1.5	15	4.6	6.1	1.6
Rb	7.9	8.4	2.8	2.0	6.9	6.7	8.0	7.3	11	11
Sr	49	63	21	9.6	17	11	32	10	116	158
Y	1.3	1.4	1.6	1.8	1.7	1.5	1.8	2.3	10	9.0
Zr	20	14	17	23	17	20	25	37	248	175
Nb	1.6	1.3	1.7	2.0	1.8	2.0	2.1	3.3	8.4	7.2
Mo	0.2	0.1	0.2	0.2	0.5	0.1	0.3	0.2	0.7	0.5
Cd	0.1	0.1	0.1	0.1	0.2	0.1	0.2	0.1	0.3	0.1
120_{Sn}	2.7	1.2	2.5	0.7	2.3	0.5	1.0	0.7	4.3	1.2
Sb	0.3	0.1	0.4	0.1	1.2	0.3	0.5	0.3	1.8	0.4
Cs	0.2	0.4	0.1	0.1	0.3	0.2	0.3	0.3	0.9	0.9
Ba	90	128	33	28	77	71	78	58	141	53
La	2.4	2.7	3.0	3.0	4.2	3.1	4.7	3.1	43	60
Ce	4.8	5.4	5.9	6.0	9.3	6.8	12	10	90	131
Pr	0.6	0.6	0.6	0.7	1.1	0.7	1.0	0.7	10	15
Nd	2.0	2.0	2.3	2.4	3.9	2.6	3.3	2.3	39	55
Sm	0.4	0.4	0.4	0.4	0.7	0.4	0.6	0.4	6.8	9.7
Eu	0.7	1.3	0.9	0.6	1.4	1.0	1.1	1.3	2.3	2.5
Gd	0.3	0.3	0.3	0.3	0.5	0.3	0.4	0.4	4.5	5.9
Dy	0.2	0.2	0.3	0.3	0.3	0.3	0.4	0.4	2.2	2.3
Ho	dl	dl	0.1	0.1	0.1	0.1	0.1	0.1	0.4	0.4
Er	0.1	0.1	0.2	0.2	0.2	0.2	0.2	0.3	1.2	1.0

Table 5. (continued)

Yb	0.2	0.1	0.2	0.2	0.2	0.2	0.2	0.3	1.3	1.0
Hf	0.5	0.4	0.5	0.6	0.5	0.5	0.8	0.9	7.0	5.0
208_{Pb}	97	173	84	6.4	1035	35	205	77	218	14
232_{Th}	0.6	0.6	0.7	0.9	0.9	0.7	1.3	1.3	13	11
238_{U}	0.2	0.2	0.2	0.2	0.3	0.2	0.3	0.3	2.4	1.8

Table 6. Compositions of the black weathering layer (BWL) and substrate (Subs) as determined by ICP-MS on partial extractions by oxalic acid. Elements in ppm; dl = detection limit.

	Z1		Z2		Z3		Z4		Z8	
	BWL	Subs	BWL	Subs	BWL	Subs	BWL	Subs	BWL	Subs
Li	0.1	0.1	0.1	0.3	0.2	0.1	0.1	dl	0.1	0.1
Na	55	8.5	33	17	24	5.8	61	20	16	6.4
Mg	14	4.8	22	5.3	16	4.7	28	6.7	18	6.7
Al	168	60	82	46	260	51	202	142	137	111
K	168	47	84	54	67	21	94	66	71	25
Ca	59	60	45	52	110	66	57	68	94	83
Sc	0.3	0.4	0.3	0.5	0.4	0.7	0.4	0.6	0.7	0.6
Ti	1.9	1.6	3.5	0.4	5.6	1.8	7.1	4.5	5.2	0.9
V	0.3	0.2	0.6	0.2	7.7	1.0	1.5	1.0	4.0	2.1
Cr	0.7	1.0	0.8	0.6	1.2	0.7	1.1	0.7	0.7	0.7
Mn	0.8	0.7	1.8	0.3	6.6	0.4	5.0	7.2	5.7	1.2
Fe	91	52	192	40	478	155	646	357	683	414
Ni	0.4	2.7	0.5	0.4	2.5	0.6	1.7	0.5	0.8	0.8
Cu	12	5.0	11	3.7	27	2.4	298	2.2	5.1	2.5
Zn	6.8	1.7	12	2.9	298	22	114	15	12	4.5
Ga	dl	dl	dl	dl	0.1	dl	0.1	dl	0.3	dl
As	0.1	0.2	dl	dl	3.2	dl	11	0.1	0.7	0.1
Rb	0.5	0.1	0.4	0.2	0.3	0.1	0.4	0.3	0.3	0.2
Sr	1.3	1.1	1.1	0.5	1.7	0.5	1.8	0.5	2.3	1.1
Y	dl	dl	dl	dl	0.2	dl	dl	0.1	0.2	0.4
Zr	1.1	0.3	0.4	0.2	0.8	0.4	0.7	0.7	1.7	1.9
Nb	0.1	0.1	0.1	dl	0.1	0.1	0.1	dl	0.1	0.1
Mo	0.1	0.2	0.1	dl	0.5	0.1	0.3	0.1	0.4	0.3
Cd	dl	dl	dl	dl	0.1	dl	dl	dl	dl	dl
120_{Sn}	1.4	0.8	1.6	0.4	1.4	0.2	0.4	0.3	1.1	0.1
Sb	dl	dl	0.1	dl	0.6	0.1	0.2	0.1	0.5	0.1
Cs	dl	dl	dl	dl	dl	dl	dl	dl	dl	dl
Ba	2.5	1.5	2.2	0.2	5.2	1.3	1.7	1.0	18	2.1
La	dl	0.1	dl	dl	0.1	dl	dl	0.1	0.1	0.1
Ce	dl	0.1	dl	dl	0.2	0.2	0.1	2.7	0.1	0.1

Table 6. (continued)

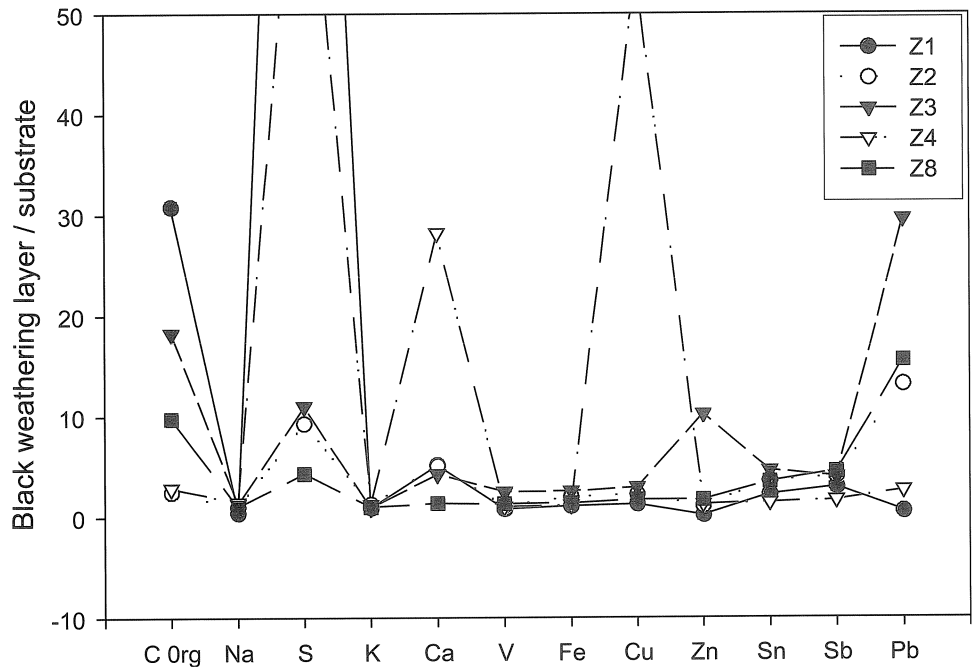|										
Pr	dl	dl	dl	dl	dl	dl	dl	dl	dl	dl
Nd	dl	0.1	dl	dl	0.1	dl	dl	0.2	0.1	0.1
Sm	dl	dl	dl	dl	dl	dl	dl	dl	dl	0.1
Eu	dl	dl	dl	dl	dl	dl	dl	dl	dl	dl
Gd	dl	dl	dl	dl	dl	dl	dl	0.1	dl	0.1
Dy	dl	dl	dl	dl	dl	dl	dl	0.1	dl	0.1
Ho	dl	dl	dl	dl	dl	dl	dl	dl	dl	dl
Er	dl	dl	dl	dl	dl	dl	dl	dl	dl	dl
Yb	dl	dl	dl	dl	dl	dl	dl	dl	dl	dl
Hf	dl	dl	dl	dl	dl	dl	dl	dl	dl	dl
208_{Pb}	5.1	110	12	0.9	374	12	20	37	58	3.0
232_{Th}	dl	0.1	dl	dl	0.1	0.1	0.1	0.2	0.3	0.2
238_{U}	dl	dl	dl	dl	0.1	dl	dl	dl	0.1	dl

Fig. 11. Enrichtment/depletion of in the black weathering layer relative to the substrate. Note that extremely enriched elements, viz. S for Z1 and Z4, and Cu for Z4, have not been plotted. For sample codes, see Table 2.

192

Table 7. Enrichment / depletion of selected elements in the black weathering layer relative to the substrate.

	Z1	Z2	Z3	Z4	Z8
Organic carbon	30.82	2.47	18.28	2.89	9.77
Na	0.43	0.98	1.28	1.48	1.02
S	142.25	9.30	11.00	76.00	4.33
K	0.95	1.27	0.95	1.25	1.00
Ca	5.17	5.10	4.25	28.2	1.38
V	0.81	1.12	2.50	0.99	1.31
Fe	1.09	1.97	2.56	1.15	1.39
Cu	1.29	2.24	2.94	54.15	1.72
Zn	0.19	1.09	10.22	1.25	1.71
Sn	2.25	3.57	4.60	1.43	3.50
Sb	3.00	4.00	4.00	1.67	4.50
Pb	0.56	13.13	29.57	2.66	15.57

7   Conclusions

Combined PFM, SEM and whole rock chemical analyses clearly demonstrate that the thin black weathering layers on Bentheim and Obernkirchen sandstone are made up by several components: gypsum, microbiota, Fe-(hydr)oxides, encapsulated airborne particles, heavy metal compounds, salts. The first four compounds are dominant, but their relative amounts vary considerably, even at the same building and at a façade with virtually the same exposure conditions.

Gypsum is a common constituent of weathering layers, and the sources of its components have been discussed widely in literature. One of the major roles of gypsum in the black weathering layers on sandstone is evidently encapsulating airborne matter (Fig. 3).

Microbiota, notably died off algae, are an important component of the black weathering layers of several samples (Fig. 5). In this aspect, the layers differ from those previously studied (e.g. Nord & Tronner 1991, 1992). However, also in the present samples, they are not always present, indicating, in part, different genetic origins for the different black weathering layers. Algae do not only contribute to the black layer by their own presence, but also by fixating airborne material. Fe-(hydroxides) are considered to be derived from solution-precipitation processes within the stone (cf. Nord & Tronner 1991, 1992). Heavy metal compounds reflect the complex history of monuments, and may be derived from several sources: air pollution, non-ferro metal building elements but also from ancient coating systems. Removal of the black weathering layer may, in the latter case, result in loss of historic information.

Removal of relatively dense weathering layers (Fig. 2), will change the hygric characteristics of the sandstones, and by consequence, of the façade as a whole. The consequences should be a part of decision making on cleaning. In addition, the role of microbiota should be considered. If conditions favouring their colonization of a façade remain unchanged, they are likely to colonize it again.

Hygric characteristics of the façade as a whole are an important parameter in this, and should be considered in decision making.

Acknowledgements

References

- Ausset, P., Lefèvre, R.A. and Monte, M. del, 2000. Early mechanisms of development of sulphated black crusts on carbonate stone. In: Fassina, V., ed., Proceedings of the 9th International Congress on the Deterioration and Conservation of Stone, Venice 1:329-337.
- Becker, U., 1987. Zur Geologie des Bentheimer Sattels (Nordteil; TK 3608, Niedersachsen); sowie petrologische, gesteinsphysikalische und bausteingeschichtliche Untersuchungen des Bentheimer Sandsteins (Valangin). Unpublished Diplomarbeit, Philipps-Universität, Marburg.
- Bluck, B.J. and Porter, J., 1991a. Sandstone buildings and cleaning problems. Stone Industries, march 1991, 21-27.
- Bluck, B.J. and Porter, J., 1991b. Aims and methods of sandstone cleaning. Stone Industries, april 1991, 21-28.
- Bommel, A.J. van, 2001. De vergrijsde (zandstenen) gevel. Unpublished memorandum, Ministerie van Volkshuisvesting.
- Chitsazian, A., 1985. Beziehung zwischen Mineralbestand, Gefüge und technologischen Eigenschaften der Niedersächsischen 'Wealden'-Sandsteine (Unterkreide). Mitteilungen Geologisches Institut der Universität Hannover 25.
- Dubelaar, C.W., 1990. A geological view of the Royal Palace, Amsterdam, Netherlands. In: Marinos & Koukis, ed., Engineering geology of ancient works, monuments and historical sites. Balkema, Rotterdam, 2057-2066.
- Dubelaar, C.W., Nijland, T.G., Linden, T.J.M. van der and Hees, R.P.J. van, 2003. Verwering en zwartverkleuring van Bentheimer en Obernkirchener zandsteen. TNO-NITG report 02-147-B.
- Dubelaar, C.W. and Pieters, J., 1992. SEM-research and X-ray microanalysis of crusts on natural stone (Royal Palace, Amsterdam, The Netherlands). Poster presentation at 7th International Congress on the Deterioration and Conservation of Stone, Lisbon.
- Esbert, R.M., Díaz-Pache, F., Alonso, F.J., Ordaz, J. & Grossi, C.M., 1992. Solid particles of atmospheric pollution found on the Hontoria limestone of Burgos cathedral (Spain). In: Proceedings of the 8th International Congress on the Deterioration and Conservation of Stone, Berlin 1:393-399.

194

- Füchtbauer, H., 1955. Zur Petrographie des Bentheimer Sandsteins im Emsland. Erdöl und Kohle 8:616-617.

- Gisbert, J., Marín-Chaves, C. & Andaluz, N., 1996. Black crusts from Rueda cloister: An approximation to fossil effects of pollution in a semi arid climate. In: Proceedings of the 8th International Congress on the Deterioration and Conservation of Stone, Berlin 1:387-392.

- Grimm, W.D., 1990. Bildatlas wichtiger Denkmalgesteine der Bundesrepublik Deutschland. Bayerisches Landesamt für Denkmalpflege, Arbeitsheft 50.

- Kemper, E., 1976. Geologischer Führer durch die Grafschaft Bentheim und die angrenzenden Gebiete (Das Bentheimer Land Nr. 64). 5th ed., Verlag Heimatverein der Grafschaft Bentheim e.V., Nordhorn.

- Krumbein, W.E., 1992. Colour changes of building stones and their direct and indirect biological causes. In: Delgado Rodrigues, J., Henriques, F. & Jeremias, F.T., ed., Proceedings of the 7th International Congress on the Deterioration and Conservation of Stone, Lisbon, 1:443-451.

- McDonnell, R.D.,Bommel, A.J. van and Kars, H., 1991. Verwering van Bentheimer zandsteen een studie naar verweerde Bentheimer zandsteen afkomstig van het gebouw van het Rijksmuseum voor Geologie en Mineralogie te Leiden en van het stadhuis te Vlaardingen. Unpublished report, Rijksgebouwendienst en Rijksdienst Oudheidkundig Bodemonderzoek.

- Nord, A.G. and Tronner, K., 1991. Stone weathering: Air pollution effects evidenced by chemical analysis. Riksantikvariämbedet, Stockholm. Konserveringstekniska Studier 4.

- Nord, A.G. and Tronner, K., 1992. Characterization of thin black layers. In: Delgado Rodrigues, J., Henriques, F. & Jeremias, F.T., eds., Proceedings of the 7th International Congress on the Deterioration and Conservation of Stone, Lisbon, 1:217-225.

- Slinger, A., Janse, H. and Berends, G., 1980. Natuursteen in monumenten. Rijksdienst voor de Monumentenzorg, Zeist / Bosch & Keuning, Baarn.

- Vendrell-Saz, M., Krumbein, W.E., Urzi, C. & Garcia-Vallès, M., 1996. Are patinas of Mediterranean monuments really related to the rock substrate ? In: Proceedings of the 8th International Congress on the Deterioration and Conservation of Stone, Berlin 1:609-624.

- Young, M., 1997. Biological growths and their relationship to the physical and chemical characteristics of sandstones before and after cleaning. PhD thesis, Robert Gordon University, Aberdeen.